ELSEVIER

Composites Science and Technology 62 (2002) 121–130

COMPOSITES SCIENCE AND TECHNOLOGY

www.elsevier.com/locate/compscitech

Prediction of the residual tensile strengths of carbon-fiber/epoxy laminates with and without interleaves after solid particle erosion

N.-M. Barkoula[a], G.C. Papanicolaou[b,*], J. Karger-Kocsis[a]

[a]*Institute for Composite Materials Ltd., University of Kaiserslautern, POB 3049, D-67653 Kaiserslautern, Germany*
[b]*Composite Materials Group, Department of Mechanical and Aeronautical Engineering, University of Patras, GR-265 00 Patras, Greece*

Received 8 February 2001; accepted 23 October 2001

Abstract

In the present work, the influence of stacking sequence, existence and position of interleaves on the solid particle erosion in carbon-fiber-reinforced epoxy composites (CFRP) was investigated. The erosive wear behavior was studied in a modified sandblasting apparatus at a 90° impact angle. The erosion behavior was considered as a repeated impact procedure (impact fatigue). A semi-empirical approach initially developed for the prediction of the residual strength after single impact was adopted and evaluated in the case of erosion conditions. The model takes into account the inherent material properties, the initial and post-impact tensile strength of the material and the visco-elastic response (mechanical damping) of the non-impacted material. The excellent agreement between theoretical predictions and experimental values corroborated the reliability of this model which may be a useful tool for the prediction of the post impact residual strength in the case of solid particle erosion. Results showed that for impact energy values lower than a characteristic threshold the damage induced does not affect the residual tensile strength after solid particle impact (erosion) of the materials. It was also established that this threshold depends on the orientation of the plies, the existence of interleaves and the energy absorption capacity of the material.

Keywords: B. Modeling; Solid particle erosion; CFRP composites; Interleaves; Stacking sequence; Residual properties

1. Introduction

Unidirectional (UD) carbon-fibre-reinforced epoxy composite (CFRP) laminates possess very high specific (i.e. density related) stiffness and strength when measured in plane. This results in the frequent use of CFRP laminates in engineering applications such as in automobile, aerospace, marine, energetics etc. [1–3]. Due to the loading situation of these applications, the composite structures have to withstand transverse (out-of-plane) low-energy impacts [4,5] and wear, abrasion and erosion [1–3,5–8]. Erosion is in analogy with repeated impact. In the case of erosion, the impact process is caused by many fast moving small particles whereas low-energy repeated impact (also called impact fatigue) is usually generated by a large mass of low velocity.

Therefore, it is very valuable to study the erosion resistance of advanced composites, to find methods to improve their resistance, to describe their property degradation and damage growth characteristics and finally to model their residual properties.

Until now the research interest was concentrated on tests performed by an instrumented falling weight or Charpy impact devices [4,5,9–25]. It is often reported that the damage tolerance of polymer composites was strongly improved by making use of the interlayering, interleaving concept (incorporation of a tough adhesive layer in the composites build-up) [14–19].

On the other hand, erosion studies on composite materials conclude a poor erosion resistance of these materials [1–3,6–8,26–29]. Erosion tests were performed under various experimental conditions (erodent flux conditions, erosive particle characteristics) on different target composites [30]. Interestingly, no information is available on the effect of interleaving on the erosion of fiber reinforced plastics. Further, the influence of stacking sequence on the erosive behavior is not fully under-

* Corresponding author.
E-mail address: gpapan@meibm.mech.upatras.gr (G.C. Papanicolaou).

0266-3538/02/$ - see front matter
PII: S0266-3538(01)00189-0

stood. Our intention was, therefore, to investigate the solid particle erosion characteristics of CFRP composites and to elucidate how the layers of the laminates and the existence and position of interleaves influence their erosion wear. A further aim of this study was to investigate the effect of these parameters on the residual tensile strength of these materials, and finally to model these properties by considering the analogy with low energy impact conditions [31].

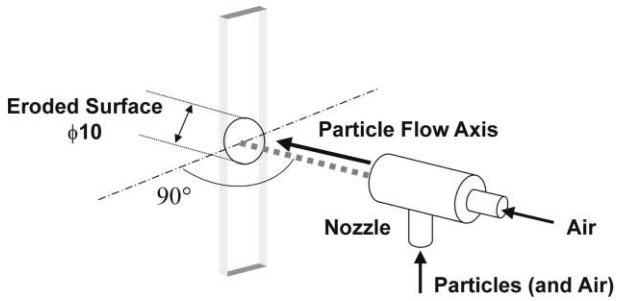

Fig. 1. Schematical representation of the test set-up used for the study of the solid particle erosion of CFRP composites.

2. Experimental

2.1. Materials

UD CFRP prepregs with thickness 0.125 mm (AS4/3501-6; BASF) were stacked in different layering (Table 1) and cured by the usual autoclave bagging according to the producer recommendation. As an adhesive interlayer (I) a modified EP (FM300, American Cyanamid) with a thickness of 0.125 mm served. The consolidation quality of all laminates was checked by ultrasonic C-scanning. Rectangular plates of 120×10 mm^2 and 60×10 mm^2 were cut from the cured laminates by a diamond saw and subjected to erosion tests. The longer specimens were afterwards subjected to tensile tests, while the shorter ones to dynamic mechanical thermal analysis (DMTA) and ultrasonic tests.

2.2. Testing methods

2.2.1. Erosion

All the erosion tests were performed in a sandblasting chamber (Fig. 1) by sharp, angular corundum with a particle size between 60 and 120 μm at 90° impact angle. The distance between the sample holder and the nozzle was constant (160 mm). Although by modifying the air pressure in the nozzle, the speed of the eroding particles can be varied, it was kept constant at 6 bar. This corresponds to a jet speed of ca. 70 m/s according to a double slat disk calibration method [32]. This resulted in a 4.08 J/s impact energy rate. All erosion tests were performed at room temperature. The eroded area was also constant as a steel cover frame with a circular opening (ϕ10) was placed on the surface of the specimens (Fig. 1).

The composite weight loss was recorded as a function of erosion time by a precision balance (AT261 Mettler Toledo, sensitivity 50μg). Before weighing, the corundum particles were removed from the specimen surface by air blasting.

Table 1
Designation and stacking sequence of the CFR-composites plates tested

Designation	Stacking sequence	Interleaf
CFRP1a	$[0_5/90_5/0_5]$	–
CFRP1I	$[0_5/I/90_5/I/0_5]$	FM300
CFRP2a	$[0_2/90_2/45_2/-45_2]_S$	–
CFRP2I	$[0_2/90_2/I/45_2/-45_2]_S$	FM300
CFRP3a	$[45_2/0_2/-45_2/90_2]_S$	–
CFRP3I	$[45_2/I/0_2/I/-45_2/90_2]_S$	FM300

2.2.2. Damage evaluation (ultrasonic scanning)

An ultrasonic C-scanning procedure was employed on the tested specimens in order to visualize the internal damages. The specimens were placed in a water tank and scanned across their surface with the help of a Panametrics 5627RPP automated ultrasonic scanning system coupled on line to a PC computer. The sensor scanning frequency was 10 MHz and scanning speed was set at 0.5 mm/s.

2.2.3. Dynamic mechanical thermal analysis (DMTA)

The viscoelastic response of both eroded and virgin laminates was studied by DMTA. An Eplexor™ 150 N (Gabo Qualimeter, Ahlden, Germany) DMTA machine was employed to carry out the tests. Rectangular specimens $60\times10\times t$ (length×width×thickness) were subjected to oscillating 3 point bending (3PB) loading composed of a static preload of 10 ± 1 N on which a sinusoidal wave of 5 ± 0.5 N at 5 Hz frequency was superimposed. Heating occurred at a rate of 1 °C/min and in a temperature range between −60 and 300 °C.

2.2.4. Tensile mechanical characteristics

Tensile properties were measured on a Zwick™ 1485, 250 kN (Ulm, Germany) universal testing machine equipped with mechanical extensometres, at a crosshead speed of 2 mm/min. All tests were performed at ambient temperature (25 ± 2 °C).

2.2.5. Failure behavior

The eroded surface was inspected in a Jeol (Tokyo, Japan) scanning electron microscope (SEM). The samples were gold-sputtered in order to reduce charging of the surface.

3. Results, discussion and modeling

3.1. Erosive wear behavior (steady state erosion)

The solid particle erosion mechanisms can be grouped in ductile and brittle categories although this grouping is not definitive [28] as a material can show both ductile and brittle behavior by changing the erosion conditions [33]. Reviewing the published results one can recognize that the failure classification of CFRP composites is biased. Häger et al. [1] claimed a semi-ductile behavior of both thermoset and thermoplastic composites under solid particle erosion by corundum particles. A different observation was made by Tsiang [9], who used aluminum oxide particles and garnet sand as abrasives. In the present study, the authors found that CFRP (AS4/3501-6) eroded brittlely. Fig. 2 displays the influence of the impact time on the erosive wear of the CFRP systems tested here. One can observe an increase of mass loss with impact time from the beginning of the experiments. This implies that the CFRP composites undergo a brittle type erosion irrespective of the layering of the laminates and the existence and position of interleaves.

The effect of the stacking sequence on the mass loss can also be deduced from Fig. 2. It seems that in non-interleaved composites a readily detectable effect is deduced and only for the case of the GF/EP3a structure. One can deduce that the 0 and 90 ° plies show the same erosion rate while the 45° plies show a greater resistance towards erosion. This observation is expected since in the case of 90° impact there is no sense to indicate the erosion direction because the particles hit the same transverse area. Accordingly the 0 and 90° plies show the same erosion rate. It is well known [1,7–8] that the failure mode in CFRP and in general in thermoset composites is a complex process involving matrix micro-cracking, fiber-matrix debonding, fiber breakage and material removal. Since the main reason for the fiber fracture is bending, when the fibers are oriented in $\pm 45°$ the part of the impact force that leads to material removal is smaller at 45° than at 0 or 90° fiber orientation. The SEM observations confirm the above mentioned mechanisms.

From Fig. 2 is also evident that the existence of interleaves had a pronounced effect on the mass loss of CFRP due to erosion. The composites with interleaves presented a much higher erosion resistance compared to that of the structures without interleaves. The difference is more pronounced in the case of the CFRP3I laminate. This hints that the position and the number of the interleaves play an important role with respect to the solid particle erosion. A first explanation for this observation is that the interleaves behave less brittle in comparison to the CF. Furthermore, the existence of the interleaves resulted in a better erosion resistance as the fiber bending due to impact is substantially reduced and the fragments of the fibers are not so easily removed due

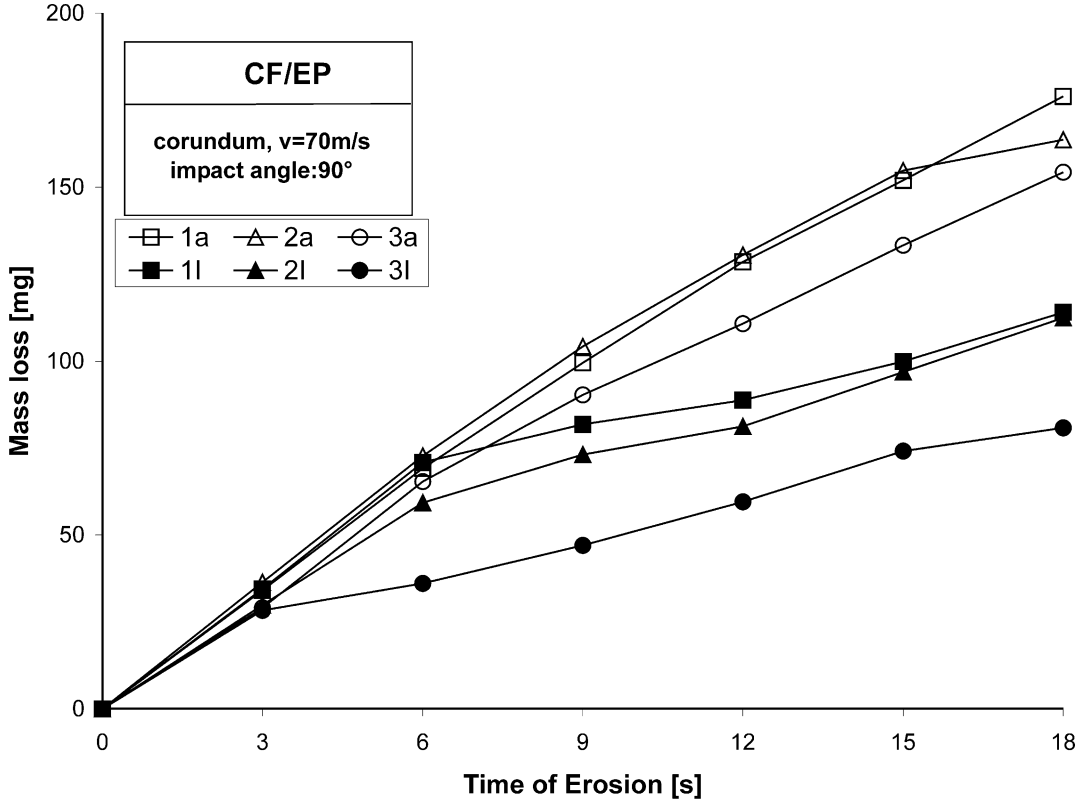

Fig. 2. Influence of erosion time, stacking sequence, existence and position of interleaves on the erosive wear of CFRP-composites.

to the better adhesion between the adjacent layers. A further effect, viz. "cushioning" of the impacted ply by the interleaf cannot be excluded either.

3.2. Damage evaluation—surface topography

Based on C-scans taken from the eroded plates after 0, 6, 12 and 18 s impact time it is observed that the damage in all cases of the materials tested was localized at the eroded area. There was no sight of delamination outside of the eroded area either in the plates with or without interleaves. Fig. 3 presents representative scans of the tested specimens.

The comparison of the Fig. 4(a–c) confirms that both stacking sequence and interleaving play an important role in solid particle erosion. In the case of the CFRP1a laminate, fiber fragmentation and matrix cracking are observed. The eroded surface of the CFRP3a composite (Fig. 4b) is less fractured while the CFRP1I [Fig. 4(c)] corroborates the above mentioned speculation that the fragments of the fibers are better bonded when interleaves are present.

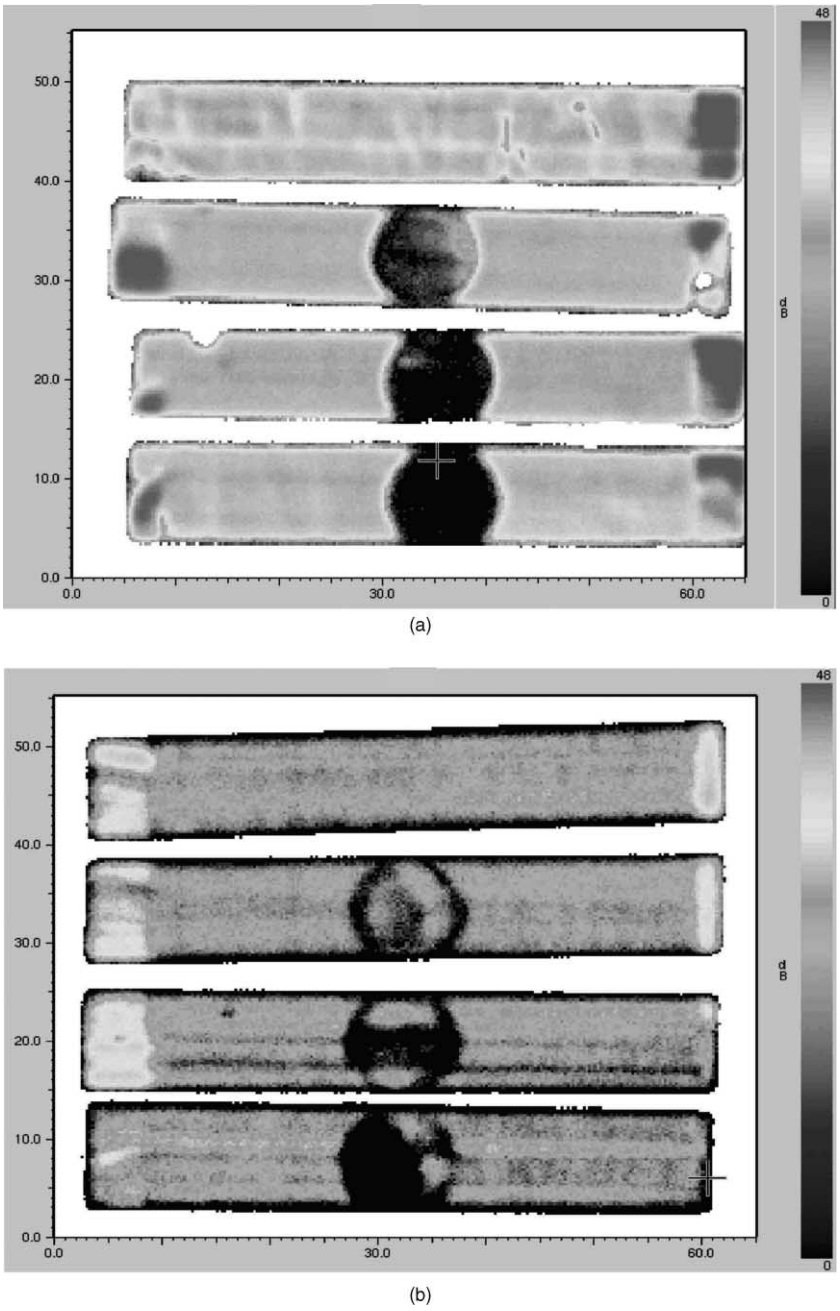

Fig. 3. Representative ultrasonic scans of the tested composites after 0, 6, 12 and 18 s erosion time: (a) CFRP1a, (b) CFRP1I.

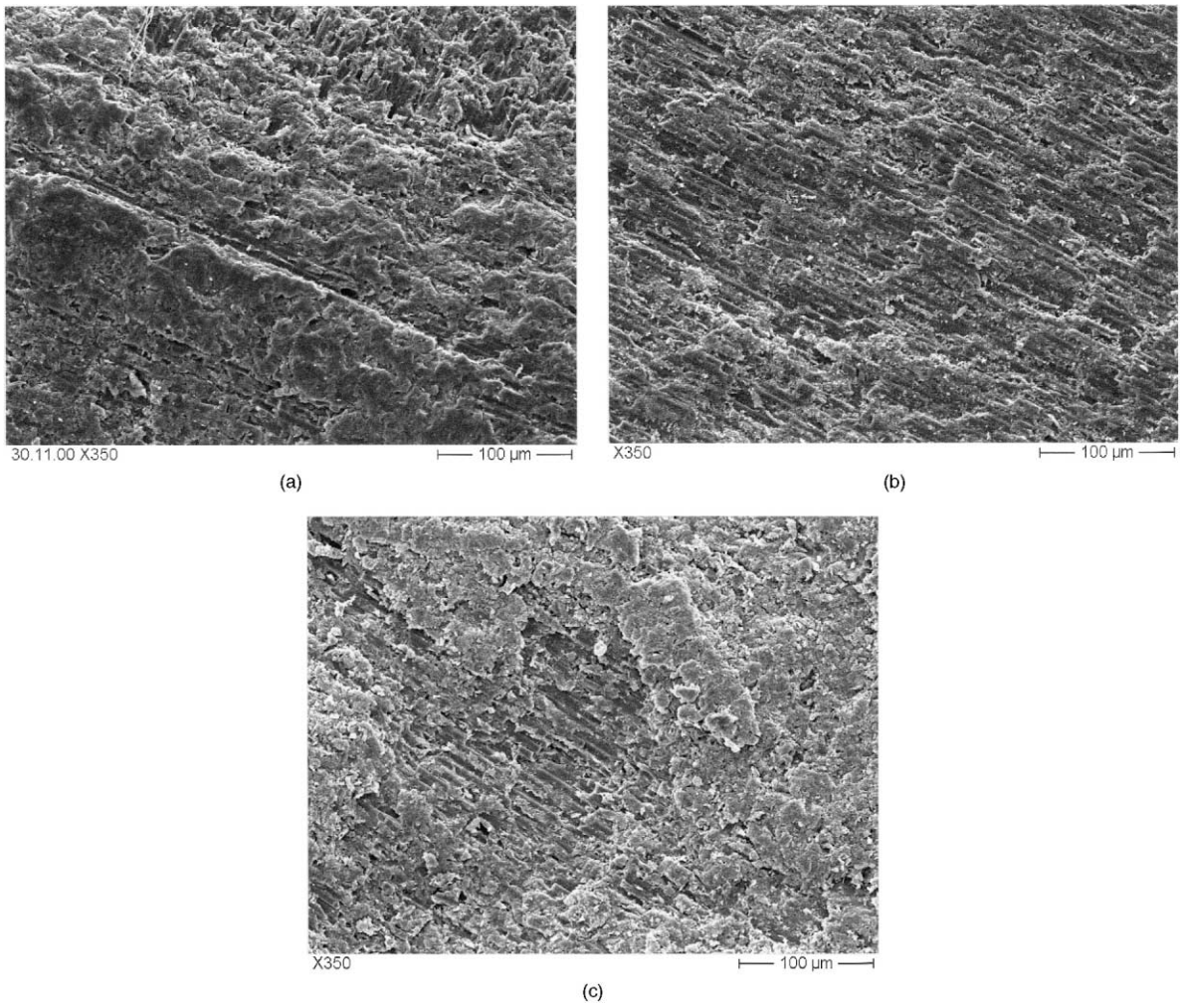

Fig. 4. Representative SEM scans of the eroded composites after 18 s erosion time: (a) CFRP1a, (b) CFRP3a and (c) CFRP1I.

3.3. Dymanic mechanical thermal analysis

DMTA spectra of the CFRP laminates before erosion are presented in Fig. 5(a and b). The reason for performing 3PB tests to the specimens is that during solid particle erosion in the range of velocities (≈70 m/s) performed here, the damage process included cracks which are associated with flexural failure [34]. Fig. 5(a) shows the variation of the storage modulus (E′) as a function of temperature whereas Fig. 5(b) presents the loss factor variation with temperature and the shifts in the glass transition (T_g) peaks of the different laminates in respect to their layering, and existence and position of interleaves.

3.4. Tensile mechanical characteristics

It is well established that when damage occurs in multidirectional CFRP laminates, broken fibres reduce the tensile strength whereas delaminations between layers reduce the compressive strength. The damage growth in solid particle erosion occurs mainly via fibre breakage and to a lesser extent through delamination. Therefore, the residual tensile strength after solid particle erosion may be a good indication of the damage state.

Table 2 resumes the experimental values of the tensile strength ratio (σ_r/σ_o, where σ_r = the residual tensile strength after impact and σ_o = the tensile strength of the non-impacted material) for different energies and laminates. As above mentioned, the solid particle erosion can be characterised as an impact fatigue procedure, which results in a stiffness reduction. Fig. 6 displays the decrease of the tensile *E*-modulus of the tested composites as a function of the impact energy. It is deduced that the laminates without $\pm 45^\circ$ oriented plies show superior stiffness. The stacking sequence does not seem to influence the *E*-modulus, before and after impact of the laminates, as the CFRP2a, CFRP3a and the CFRP2I, CFRP3I show almost the same stiffness degradation. The existence of the interleaves leads to structures with reduced stiffness especially at low impact energies.

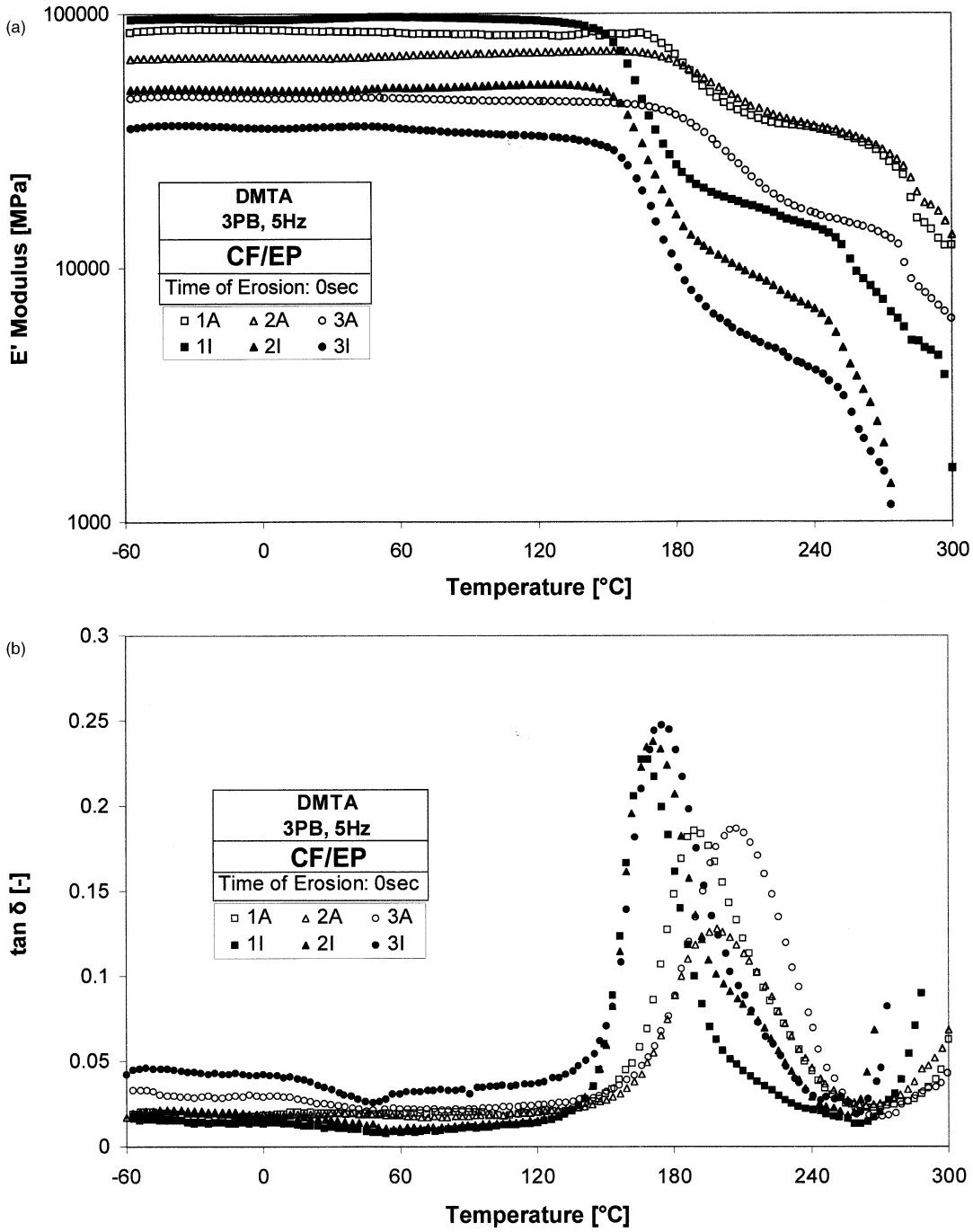

Fig. 5. DMTA spectra of the CFRP laminates before erosion (a) storage modulus (E'), (b) loss factor (tanδ).

3.5. Modeling of the residual tensile strength after impact

Papanicolaou et al. [20–25] adopted an approach to describe the residual strength of impacted fiber reinforced (FRP) laminates. However, a limitation of that model was its prerequisite of evaluating laminates including always $\pm 45^{\circ}$ oriented plies. In order to overcome this limitation, a new model was recently developed by Papanicolaou which takes into account the quasi-static response of the impacted structures. The theoretical background of this model is analytically described elsewhere [31].

Visco-elastic behavior of fiber and matrix materials is not the only mechanism for the structural damping in composite materials but appears to be the dominant mechanism in undamaged polymer composites vibrating at small amplitudes. This is also the case in solid particle erosion.

The degradation of the mechanical strength due to impact damage is assumed to follow an exponential decay law of the form:

$$\frac{\sigma_r}{\sigma_o} = 1 - e^{-u} \tag{1}$$

where u is a function of the impact energy as well as of the energy absorption capacity of the material expressed through $\tan\delta$.

Thus, the strength degradation after low energy impact can be described by a differential equation of the type:

$$s = y + \left[\frac{1-s}{s}\right]\frac{dy}{dx} \tag{2}$$

where: $s = \frac{\sigma_\infty}{\sigma_o}$ = residual tensile strength at high impact energy/tensile strength before impact

$$y = \frac{\sigma_r}{\sigma_o}$$

$$x = \frac{\Delta U}{U_o} = \frac{U - U_o}{U_o}$$

where

U = the impact energy

U_o = the impact energy threshold related to the onset of strength degradation. For impact energy values $U \leqslant U_o$, no interior damage is induced; the impact energy causes the laminate to deform elastically. Once the impactor ceases to exert load on the plate, the latter recovers its original shape and retains its nominal strength in compression/tension.

Solving Eq. (2) we obtain:

Table 2
Experimental values of the tensile strength ratio (σ_r/σ_o), for different impact energies and laminates

	CFRP1a	CFRP2a	CFRP3a	CFRP1I	CFRP2I	CFRP3I
	σ_o = 841 (MPa)	σ_o = 623 (MPa)	σ_o = 533 (MPa)	σ_o = 750 (MPa)	σ_o = 550 (MPa)	σ_o = 450 (MPa)
U (J)	σ_r/σ_o	σ_r/σ_o	σ_r/σ_o	σ_r/σ_o	σ_r/σ_o	σ_r/σ_o
12.24	0.870	0.383	0.861	1.025	0.545	1.016
24.48	0.647	0.422	0.398	0.741	0.455	0.872
36.72	0.452	0.389	0.433	0.798	0.396	0.591
48.96	0.410	0.434	0.412	0.772	0.409	0.459
61.2	0.392	0.407	0.377	0.865	0.398	0.414
73.44	0.390	0.406	0.375	0.780	0.333	0.326

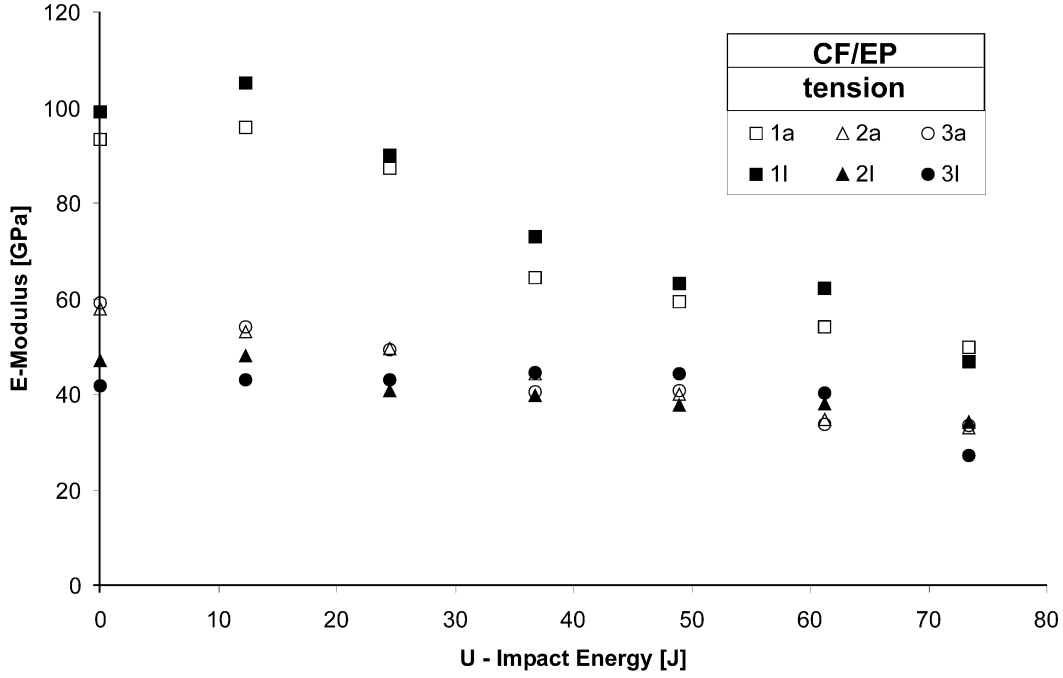

Fig. 6. Variation of the tensile E-modulus, versus impact energy, U.

$$\frac{\sigma_r}{\sigma_o} = 1 - (1-s)\left[1 - \exp\left(-\frac{s}{1-s}\frac{\Delta U}{U_o}\right)\right] \quad (3)$$

From physical considerations, the value of the strength degradation impact energy threshold, U_o, can be calculated by:

$$U_o = U_{elastic}\frac{\tan\delta}{m(1-s)} = \frac{\sigma_o^2}{2E_{11}}V\frac{\tan\delta}{m(1-s)} \quad (4)$$

where:

E_{11} = is the effective longitudinal Young' s modulus of the laminate,

V = the total volume of the specimen

$\tan\delta$ = loss factor at the T_g of the non-impacted material.

m = is the mismatching coefficient between adjacent layers due to the difference in their fiber orientation angle [20–25], defined as follows:

$$m = \frac{\sum_{\kappa=1}^{n}(\overline{M}_\kappa)_0[Q_{xx,\kappa}(z_\kappa^3 - z_{\kappa-1}^3)]}{\sum_{\kappa=1}^{n}[Q_{xx,\kappa}(z_\kappa^3 - z_{\kappa-1}^3)]} \quad (5)$$

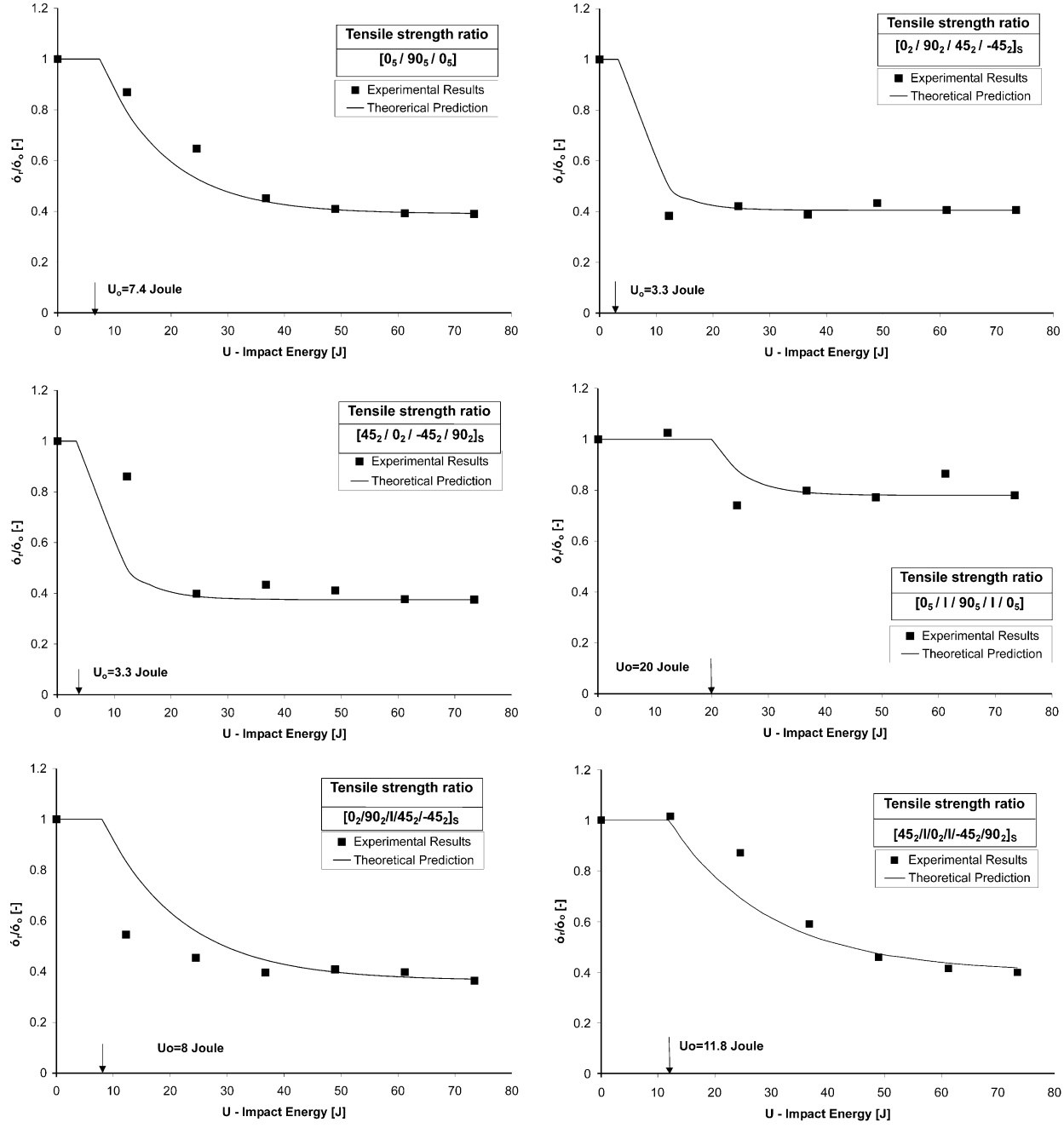

Fig. 7. Variation of the normalised residual tensile strength, (σ_r/σ_o), versus impact energy, U and comparison to respective model predictions. (a) CFRP1a, (b) CFRP2a, (c) CFRP3a, (d) CFRP1I, (e) CFRP2I and (f) CFRP3I.

Table 3
Parameters used and derived by applying the proposed model to CFRP laminates

	σ_o (MPa)	σ_∞ (MPa)	s (−)	m (−)	Tanδ (−)	V (mm3)	E_{11} (GPa)	U_o (J)
CFRP1a	841	328	0.390	0.181	0.185	1125	90	7.4
CFRP2a	623	253	0.406	0.259	0.128	1200	59	3.3
CFRP3a	533	200	0.375	0.259	0.187	1200	59	3.3
CFRP1I	750	585	0.780	0.168	0.227	1275	110	20
CFRP2I	550	200	0.364	0.257	0.238	1350	47.6	8
CFRP3I	450	180	0.400	0.110	0.248	1500	46.5	11.8

Here $(\overline{M_\kappa})_0$ is the mean value for the bending stiffness mismatching coefficient of the κ-lamina, $Q_{xx,\kappa}$ is the x-direction stiffness matrix term of the κ-lamina, z_κ is the distance of the κ-lamina from the middle plane of the laminate and n is the total number of plies in the laminate. The mean value of $(\overline{M_\kappa})_0$ is defined as follows:

$$(\overline{M_\kappa})_0 = \frac{(M_{\kappa-1,\,\kappa})_0 + (M_{\kappa,\,\kappa+1})_0}{2} \tag{6}$$

where $(\overline{M_\kappa})_0$ refers to κ-lamina and $M_{\kappa-1,\,\kappa}$ and $M_{\kappa,\,\kappa k+1}$ refer to the interfaces of the adjacent layers $(\kappa-1)$, κ and κ, $(\kappa+1)$.

The above-mentioned m-parameter depends on the laminate material system elastic properties, layering, stacking sequence and individual lamina thickness.

3.6. Model verification

In order to apply this semi-empirical model three test series are needed. Two tensile tests in order to determine σ_o and σ_∞ and one DMTA test to define tanδ of the non-impacted specimen.

Table 3 presents all the characteristic of the materials used as well as their energy threshold as derived from the model. The values of σ_o, σ_∞, E_{11} and tanδ are experimentally defined. Applying Eqs. (3) and (4) of the proposed model, the parameters s and U_o, are calculated. For calculating m, the following elastic constants of the used CFRP system were considered: $E_1 = 138$ GPa, $E_2 = 8.96$ GPa, $G_{12} = 7.1$ GPa, and $v_{12} = 0.3$. For the interleaves the respective values are $E_1 = 3.35$ GPa, $E_2 = 3.35$ GPa, $G_{12} = 1.29$ GPa, and $v_{12} = 0.3$.

Taking into account the U_o values as derived from Eq. (4), a comparative study between experimental data and theoretical predictions was carried out. Plotting the tensile strength ratio σ_r/σ_o, versus impact energy, U (Fig. 7), it can be noted that the proposed model seems to predict well both the impact energy threshold and the tensile strength ratio for all CF/EP laminates studied.

It is interesting to note that the impact energy threshold is higher in the case of the cross-ply laminates and in the case of systems with interleaves. It is also observed that the reduction rate of the residual after impact strength in the case of the cross-ply laminates, with or without interleaves, is smaller in comparison to all other systems.

4. Conclusions

Based on the present study performed on the solid particle erosion of interleaved and non-interleaved CFRP composites with various stacking sequences the following conclusions can be drawn:

1. The CFRP systems undergo brittle erosion. Both stacking sequence and interleaves affect the erosion resistance of these composites. The incorporation of $\pm 45^\circ$ oriented plies as well as of interleaves leads to composites with superior erosion resistance.
2. The solid particle erosion can be handled as a repeated low energy impact procedure. The damage growth under erosion is therefore likely similar to that of impact fatigue.
3. A new model for the prediction of the residual strength after impact was evaluated. The model predicts both the impact energy threshold and the residual strength after solid particle impact. The proposed model seem to be a promising design tool since it can be applied to any type of impacted material and for its application a minimum number of experimental input data is needed.

Acknowledgements

This work was supported by the German Science Foundation (DFG Ka 1202/6-1).

References

[1] Häger A, Friedrich K, Dzenis Y, Paipetis SA. Study of erosion wear of advanced polymer composites. In: Street K, editor. ICCM-10 Conference Proceedings, Whistler, B.C., Canada. Cambridge (UK): Woodhead Publishing, 1995.
[2] Tilly GP. Sand erosion of metals and plastics: a brief review. Wear 1969;14:241–8.
[3] Tilly GP. Erosion caused by airborne particles. Wear 1969;14:63–79.

[4] Cantwell WJ, Morton J. The impact resistance of composite materials: a review. Composites 1991;22:347–62.
[5] Choi HY, Downs RJ, Chang F-K. A New approach towards understanding damage mechanisms and mechanics of laminated composites due to low-velocity Impact: part I—Experiments. Journal of Composite Materials 1991;25:992–1011.
[6] Miyazaki N, Takeda N. Solid particle erosion of fiber reinforced plastics. Journal of Composite Materials 1993;27(1):21–31.
[7] Pool KV, Dharan CKH, Finnie I. Erosion wear of composite materials. Wear 1986;107:1–12.
[8] Zahavi Jr. J, Schnitt GF. Solid particle erosion of reinforced composite materials. Wear 1981;71:179–90.
[9] Nagai M, Miyairi H. The study on Charpy impact testing methods of CFRP. Advanced Composite Materials 1994;3:17–190.
[10] Tai NH, Yip MC, Lin JL. Effects of low-energy impact on the fatigue behavior of carbon/epoxy composites. Composites Science and Technology 1998;58:1–8.
[11] Hitchen SA, Kemp RM. The effect of stacking sequence on impact damage in a carbon fiber/epoxy composite. Composites 1995;26(3):207–14.
[12] Abrate S. Impact on laminated composites: recent advances. Applied Mechanics Reviews 1994;47(11):517–44.
[13] Strait LH, Karasek ML, Amateau MF. Effects of stacking sequence on the impact resistance of carbon fiber reinforced thermoplastic toughened epoxy laminates. Journal of Composite Materials 1992;26(12):1725–39.
[14] Sela N, Ishai O. Interlaminar fracture toughness and toughening of laminated composite materials: a review. Composites 1989;20: 423–35.
[15] Sela N, Ishai O, Banks-Sills L. The effect of adhesive thickness on interlaminar fracture toughness of interleaved CFRP specimens. Composites 1989;20:257–64.
[16] Lu WH, Liao FS, Su AC, Kao PW, Hsu TJ. Effect of interleaving on the impact response of a unidirestional carbon/epoxy composite. Composites 1995;26(3):215–22.
[17] Yuan Q, Karger-Kocsis J. Effects of interleaving on the impact and impact fatigue responses of cross-ply carbon fiber/epoxy laminates. Polymers and Polymer Composites 1995;3(3):171–9.
[18] Yuan Q, Friedrich K, Karger-Kocsis J. Low-energy charpy impact of interleaved CF/EP laminates, part I. Effects of interleaving on stiffness degradation. Applied Composite Materials 1995;2:119–33.
[19] Yuan Q, Karger-Kocsis J. On the efficiency of interleaves in carbon fiber/epoxy composite laminates by the fractal approach. Journal of Materials Science Letters 1996;15:842–5.
[20] Papanicolaou GC, Stavropoulos CD. New approach for residual compressive strength prediction of impacted CFRP laminates. Composites 1995;26(7):517–23.
[21] Stavropoulos CD, Papanicolaou GC. Effect of thickness on the compressive performance of balistically impacted CFRP laminates. Journal of Materials Science 1997;32:931–6.
[22] Papanicolaou GC, Stavropoulos CD, Mouzakis DE, Karger-Kocsis J. Residual tensile strength modelling of polymer–polymer microlayer composites after low energy impact. Plastics Rubber and Composites, Processing and Applications 1997;26(9):412–7.
[23] Papanicolaou GC, Blanas AM, Pournaras AV, Stavropoulos CD. Impact damage and residual strength of FRP composites. In Kim JK, Yu TX, editors. Key engineering materials, impact response and dynamic failure of composites and laminate materials, Part 1: impact damage and ballistic impact. Trans Tech Publications 1998;141–143:127–48.
[24] Stavropoulos CD, Papanicolaou GC, Karger-Kocsis J, Mouzakis DE. Effect of $\pm 45^{\circ}$ layers on the residual compressive strength of impacted glass fibre/polyester laminates. In: Gibson, AG, ed. FRC Seventh International Conference on Fibre Reinforced Composites Conference Proceedings 15–17, April 1998, Newcastle upon Tyne, 1998. p. 327–37.
[25] Papanicolaou GC, Pournaras AV, Mouzakis DE, Karger-Kocsis J, Bofilios, DA. Probabilistic approach for residual compressive strength of CFRP laminates after low velocity impact. In: Reifsnider KL, Dillard DA, Cardon AH, editors. Progress in Durability Analysis of Composite Systems. Balkema, Rotterdam, 1998. p. 325–330.
[26] Tilly GP, Sage W. The interaction of particle and material behaviour in erosion process. Wear 1970;16:447–65.
[27] Miyazaki N, Hamao T. Effect of interfacial strength on erosion behavior of FRPs. Journal of Composite Materials 1996;30:35–50.
[28] Tsiang TH. Sand erosion of fiber composites: testing and evaluation. In: Chamis CC, editor. Test methods for design allowables for fibrous composites. 2 ASTM STP 1003, American Society for Testing and Materials, Philadelphia, 1989. p. 55–74.
[29] Roy M, Vishwanathan B, Sundararajan G. The solid particle erosion of polymer matrix composites. Wear 1994;171:149–61.
[30] Finnie I. Some reflections on the past and future of erosion. Wear 1995;186-187:1–10.
[31] Papanicolaou GC. A New model for the prediction of the residual strength after impact of laminated composites. Composites Science and Technology (in press).
[32] Ruff AW, Ives LK. Measurement of solid particle velocity in erosive wear. Wear 1975;35:195–9.
[33] Hutchings I. Ductile-brittle transitions and wear maps for the erosion and abrasion of brittle materials. Journal of Physics D: Applied Physics 1992;25:A212–0A221.
[34] Dorey G. Fracture behaviour and residual strength of carbon fibre composites subjected to impact loads. In: Failure modes of composite materials with organic matrices and their consequences on design. AGARD Conference Proceedings No.163, 1975. Paper 8.